

Controlling spin-polarized electron transport through a molecule: The role of molecular conformation

L. Senapati,¹ R. Pati,² and S. C. Erwin^{1,*}¹Center for Computational Materials Science, Naval Research Laboratory, Washington, DC 20375, USA²Department of Physics and Multi-Scale Technology Institute, Michigan Technological University, Houghton, Michigan 49931, USA

(Received 14 August 2006; revised manuscript received 22 November 2006; published 31 July 2007)

We investigate theoretically the spin-polarized electron transport through a complex organic molecule coupled to magnetic contacts. Our focus is on how low-energy deformations of the molecule affect the current-voltage characteristics and the magnetotransport of this molecular-scale device. We find that fairly modest deformations, costing only a few tens of meVs, can substantially change the tunneling current—by factors of 2 or more. Such deformations have still larger impact on the magnetoresistance, with small changes in molecular conformation even leading to changes in the sign of the magnetoresistance.

DOI: 10.1103/PhysRevB.76.024438

PACS number(s): 75.10.Jm, 03.67.Lx, 03.67.Pp

I. INTRODUCTION

The field of molecular electronics offers one possible solution to the problems faced by silicon technology as device miniaturization continues into the nanoscale regime.^{1–8} Some of the most interesting recent research in this field addresses the creation and detection of spin-polarized electron transport through a variety of molecular-scale conductors, including single and multiwalled carbon nanotubes,⁹ semiconductor quantum dots connected by a molecular bridge,¹⁰ organic thin films,¹¹ and self-assembled organic monolayers.¹² Organic molecules and films are especially promising building blocks for spin-polarized molecular electronic devices because the spin-coherence length can be much larger than in metals and traditional semiconductors. Of course, achieving large spin-coherence lengths require using thin films in which transport is controlled by just a few layers of molecules. Moreover, the spin-orbit interaction and spin-flip scattering are generally weak in organic molecular systems, an important advantage for applications in molecular spintronics.

There have been several theoretical efforts aimed at understanding how electron transport through a molecular junction is affected by the relative magnetic alignment of its two metallic contacts.^{13–21} Many of these calculations showed that by changing the magnetic alignment of the contacts one could substantially affect the electronic current in the molecular circuit. In one example—a single benzene-1,4-dithiolate (BDT) molecule between two Ni clusters—parallel magnetic alignment led to significantly higher current (by one order of magnitude) than antiparallel alignment, suggesting the possibility of a molecular spin valve.¹⁵ Indeed, recent experimental progress in measuring magnetotransport properties in organic thin films¹¹ and in self-assembled organic monolayers¹² shows that measurement of spin-polarized transport in single molecules is not far off.

One interesting, yet unresolved, issue regarding these findings is the role played by the molecular bridge itself in the spin-polarized electron transport. Even in the absence of the molecule, one would observe spin-dependent electron tunneling between two magnetic contacts placed in close proximity. The extent to which the physical and electronic

structure of an intervening molecule also affect the electron transport is not obvious. In this paper, we address this issue by investigating the role of a non-magnetic molecular bridge in the spin-polarized electron transport between two magnetic contacts. Specifically, we ask to what extent low-energy deformations of the geometrical conformation of the molecule control its transport properties.

We address this question using the simple, yet physically plausible, example shown in Fig. 1. The complete system consists of a single 1,12-tri-benzene-dithiolate (TBDDT) molecule attached between two magnetic nickel contacts, which are themselves attached to semi-infinite gold leads. The TBDDT molecule itself is a short molecular chain consisting of three benzene molecules, linked by single C-C bonds and terminated by sulfur atoms at either end. The sulfur atoms help to anchor the molecule to the metal contact. Each Ni contact consists of a cluster of three Ni atoms. Using such a small cluster makes the formation of magnetic domains less likely than in larger clusters; in practice we find this strategy works well.

To calculate the spin-polarized current-voltage (I - V) characteristics of the TBDDT molecular bridge, we use density-functional theory²² and the Landauer-Büttiker multi-channel formalism.²³ The low-energy conformational deformations that we consider here are rotations of the central benzene molecule about the TBDDT long axis. In the ground state of the system, the central molecule is rotated about this axis by approximately 40°, relative to the plane of the neighboring benzene molecules. We investigate rotation angles from 40° to zero, ultimately forcing the TBDDT molecule into a higher-

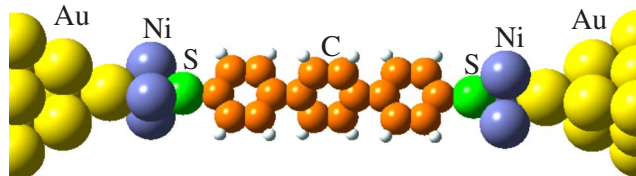


FIG. 1. (Color online) A single 1,12-tri-benzene-dithiolate (TBDDT) molecule attached between two magnetic nickel contacts (blue). Semi-infinite gold contacts (yellow) are represented in the calculation by single “dressed” atoms.

energy coplanar conformation. For each angle we calculate the I - V characteristics for both parallel and antiparallel alignment of the magnetic Ni contacts.

As described in detail below, we find that the magnetoresistance is very sensitive to the conformation of the TBDT molecular bridge. In the ground-state conformation, the total current is higher for antiparallel Ni alignment than for parallel alignment. However, by forcing the TBDT into a coplanar conformation this relationship is reversed, with the current now higher for parallel Ni alignment. Thus, we find that even the sign of the magnetoresistance can be changed by deformation in the molecular conformation.

The rest of the paper is organized as follows. Our theoretical methods are described in Sec. II, followed by the results and discussion in Sec. III. Section IV summarizes our main results with a brief conclusion.

II. THEORETICAL METHODS

For computational purposes we partition the system shown in Fig. 1 into two regions. The first region consists of the TBDT molecule plus the two Ni clusters representing the magnetic contacts. The second region consists of the two semi-infinite Au leads, each of which we represent using a single “dressed” Au atom. The left and right Ni clusters act as a spin polarizer and analyzer, respectively. We used density-functional theory (DFT) (Ref. 22) to calculate the ground-state physical and electronic structure of the TBDT molecule attached to the two Ni clusters.

The DFT calculations were performed in the gradient-corrected local-spin-density approximation with Becke’s three-parameter hybrid functional B3LYP, which includes Hartree-Fock exchange and Lee-Yang-Parr exchange and correlation functionals, as implemented in GAUSSIAN 03.²⁴ We used all-electron 6-311+G* basis functions for carbon, sulfur, and hydrogen atoms, and LANL2DZ (Los Alamos effective core potential with double zeta) basis sets for Ni and Au. The convergence criterion for self-consistency of the total energy was taken as 10^{-8} Hartree.

The transport calculations were carried out in the regime of low bias, using the multi-channel formalism of Landauer-Büttiker based on the Green’s function.²³ We neglect the effects of incoherent and spin-flip scattering because spin-orbit and hyperfine interactions in this molecular system are weak. Hence, the total current is simply the sum of spin-up (\uparrow) and spin-down (\downarrow) currents:

$$I^{\uparrow,\downarrow}(V_b) = \frac{e}{h} \int_{\mu_1}^{\mu_2} T^{\uparrow,\downarrow}(E, V_b) [f(E - \mu_2) - f(E - \mu_1)] dE. \quad (1)$$

The limits of integration are the electrochemical potentials of the Au contacts, μ_1 and μ_2 , under the applied bias voltage, V_b . For the strongly coupled molecular system we are considering, the potential drop is expected to be equally distributed between the left and right contacts. Thus the electrochemical potentials can be taken to be $\mu_1 = E_f - eV_b/2$ and $\mu_2 = E_f + eV_b/2$, where E_f is the bulk Fermi energy for Au. E is the injection energy of the electrons and f is the Fermi distribution function.

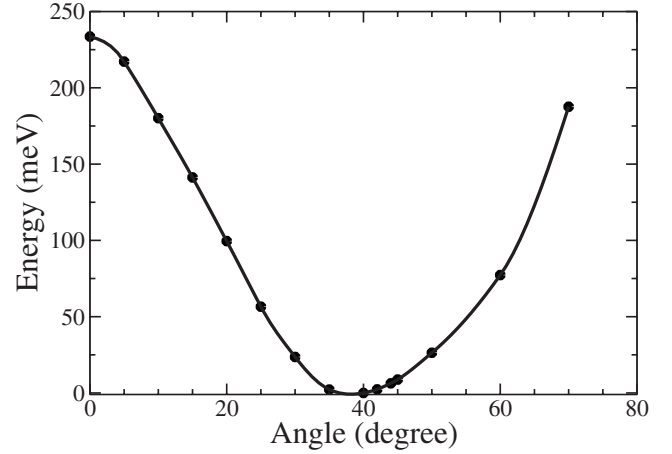


FIG. 2. Variation of the total energy of the TBDT molecule as the central benzene molecule is rotated rigidly about the long molecular axis. The ground state geometry is at approximately $\theta = 40^\circ$.

The transmission function $T^{\uparrow,\downarrow}$ appearing in Eq. (1) represents the sum of transmission probabilities for electrons transmitted through the molecule, and is calculated from the Green’s functions.^{15,23} The Green’s function (G) is evaluated from the effective Hamiltonian of the extended molecule (H) and self-energy functions (Σ) as $G = [EI - H - \Sigma_L - \Sigma_R]^{-1}$. The self energy functions for left (L) and right (R) leads are defined as $\Sigma_{L(R)} = [c_{L(R)} g_{L(R)} c_{L(R)}^\dagger]$, where we have used the dressed gold atoms to obtain the coupling matrices (c). Finally, we have used the local density of states (0.035 states/eV-spin) of the 6s band of bulk gold to approximate the Green’s function (g) of the (bulk) Au contact.^{23,25,26}

III. RESULTS AND DISCUSSION

A. Structure and energetics of molecular region

We begin by determining the ground-state structure of the TBDT molecular region described in Sec. II. Initially, we take the two Ni contacts to have parallel magnetic alignment. In the resulting equilibrium geometry we find that the central benzene ring is rotated by approximately $\theta = 40^\circ$ relative to the plane of the neighboring benzene rings. To study deformations away from this minimum we performed a series of calculations, each with fixed molecular geometry, in which the central benzene molecule was rotated rigidly about the long molecular axis. Figure 2 shows the resulting variation of the total energy with rotation angle. The energy difference between the ground state ($\theta = 40^\circ$) and the co-planar conformation ($\theta = 0^\circ$) is 230 meV. This is much larger than the thermal energy available at room temperature. In the next section, we return to the question of the extent to which such conformational changes can be induced by applying an external field.

B. Transport

Using the Landauer-Büttiker approach described in Sec. II, we calculated the I - V characteristics for several different

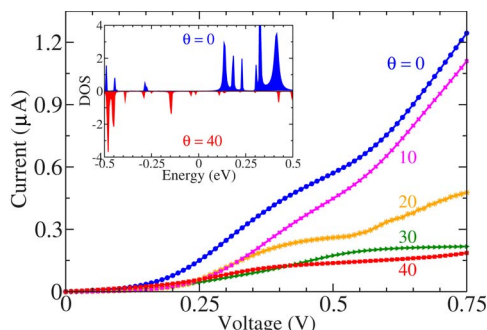


FIG. 3. (Color online) Current-voltage characteristic of the molecular device shown in Fig. 1, for different rotation angles θ of the central benzene molecule, for the case of parallel magnetic alignment of the Ni contacts. Inset: Total density of states (DOS), for the two extreme cases $\theta=0$ and 40° , near the Fermi level (zero of energy).

rotation angles θ . We discuss first the case of parallel magnetic alignment of the Ni contacts. The results for five different values of θ are shown in Fig. 3.

Two comments are in order. First, the current is generally largest when the TBDT molecule is constrained to the coplanar conformation ($\theta=0$). Except at very low bias (below 0.2 V), the current is reduced as the angle is increased, and reaches its minimum value at the equilibrium geometry ($\theta=40^\circ$).

To understand this variation of the current with angle, we have analyzed the density of states (DOS) near the Fermi level for the two extremal cases, $\theta=0$ and 40° , focusing on bias values larger than 0.2 V. As shown in Fig. 3, the planar conformation leads to a significantly larger DOS near the Fermi level than does the ground-state conformation. The origin of this increased DOS is the strong σ - π conjugation found in the planar conformation, which provides efficient pathways for electron transport. Rotating the central benzene ring breaks the σ - π conjugation, resulting in a reduced current. As shown in Fig. 4, the highest-occupied-molecular-orbital (HOMO) and lowest-unoccupied-molecular-orbital (LUMO) plots strongly establish the breaking of π conjugation by rotating the central benzene ring. The transport is mainly channeled through the LUMO, where the p orbital of the sulfur is strongly hybridized with the p orbital of the carbon, as well as the d orbital of Ni. However, the difference in current in these two extreme cases can be better understood by investigating the localization of the orbital in the backbone of the 3-benzene rings. It is evident from the orbital plots that the increase/decrease in current depends on the localization of orbital states on the backbone of the molecule. The rotation of the central benzene in the off-planar configuration weakens the π -coupling (the π -overlap being dependent upon the cosine of the rotation angle) between the central and terminal benzene ring as evident from the LUMO plot. This leads to the reduction in the current for the non-planar configuration.

Similar conformational effects have been shown theoretically in π - σ - π molecular wires,²⁷ and have also been observed experimentally in porphyrin (Cu-TBPP) molecules.²⁸

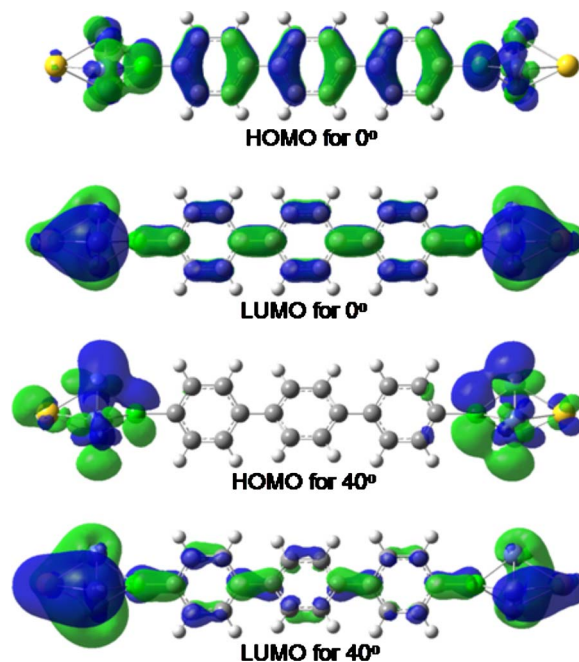


FIG. 4. (Color online) HOMO-LUMO plots for the two extreme cases $\theta=0$ and 40° of parallel spin configuration. Blue(black) and green(gray) are used to indicate the positive and negative sign of the wave function. From these HOMO-LUMO plots, it is evident that the current is mainly controlled by the overlap of molecular orbitals on backbone of the molecule.

Very recently, conformational changes created by STM tips in azobenzene molecules have been observed to lead to switching behavior.²⁹ Similar variations in the I - V characteristics of long chain molecules, arising from vibrational modes, have also been observed.³⁰

Second, we see in Fig. 3 that for angles near equilibrium the current essentially saturates for voltages between 0.5–0.75 V, while for angles near the coplanar deformed geometry the current continues to rise with voltage. This behavior has the interesting consequence that for voltages between 0.5–0.75 V there is nearly an order of magnitude difference in the current for $\theta=0$ compared to $\theta=40^\circ$, suggesting the

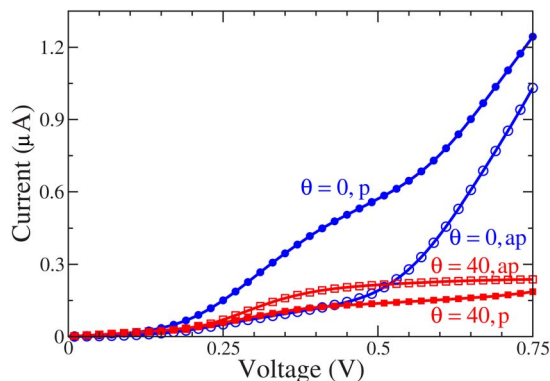


FIG. 5. (Color online) Comparison of I - V characteristics for parallel (P) and antiparallel (AP) magnetic alignments of the Ni contacts, for $\theta=0^\circ$ and $\theta=40^\circ$.

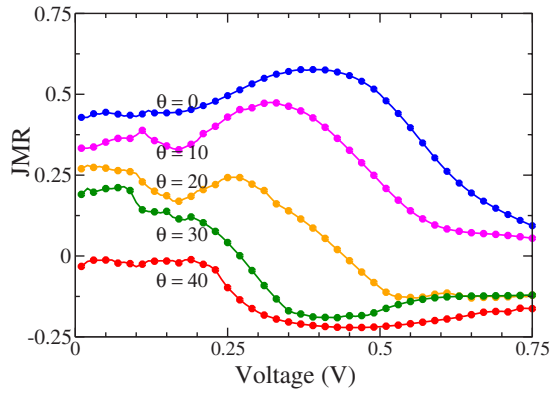


FIG. 6. (Color online) Calculated junction magnetoresistance as a function of voltage and rotation angle.

possibility of using conformational changes to control a molecular variable resistor (potentiometer). The energy required to create this particular deformation is ~ 230 meV, much larger than the typically available thermal energy. One possible way to create such a deformation is with an applied electric field. As an example, we find that an applied electric field of 0.5×10^6 V/cm perpendicular to the molecular axis changes the equilibrium value of θ by about 5° .

We now compare the transport behavior for parallel and antiparallel alignment of the magnetic Ni contacts. A comparison of the I - V characteristics for parallel and antiparallel alignment is shown in Fig. 5 for two extremal cases, $\theta=0$ and 40° . For $\theta=0$ the current for antiparallel alignment is smaller than for parallel alignment. For $\theta=40^\circ$ the situation is reversed: the current for antiparallel alignment is now larger than for parallel alignment. This reversal of current can be understood from the inspection of the coupling between Ni and S, and between S and C atoms. In contrast to the planar configuration, for the non-planar configuration, the couplings between the d state of Ni and p state of S, and between the p orbitals of S and C are stronger in the antiparallel configuration than that in the parallel configuration. This leads to an increase in current in the case of off-planar antiparallel configuration.

To quantify this behavior in more detail, we define the junction magnetoresistance ratio (JMR) at each voltage as

$$\text{JMR} = \frac{I_P - I_{AP}}{(I_P + I_{AP})/2}, \quad (2)$$

where I_P and I_{AP} are the total currents for parallel and antiparallel magnetic alignment, respectively.¹⁹ Figure 6 shows the resulting JMR as a function of voltage, for several rotation angles θ . The JMR is generally largest (more positive) for the most coplanar conformations, becoming smaller—and eventually negative—as the rotation angle approaches its equilibrium value. There is also a sizable dependence of the JMR on voltage for all angles.

To characterize the crossover of the JMR from positive to negative in more detail, we have computed the conductance (dI/dV) as a function of θ , using the low-bias linear regime of our calculated I - V curves. Figure 7 shows how dI/dV

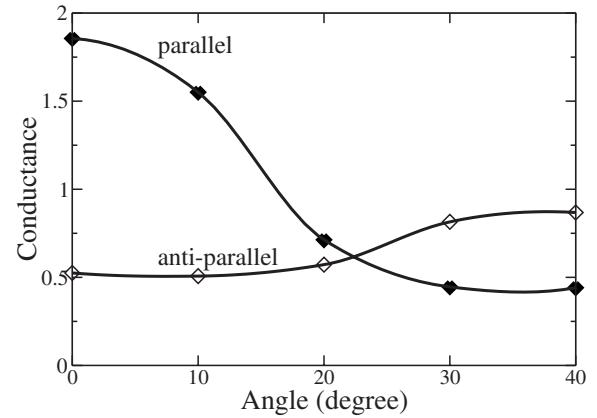


FIG. 7. Conductance as a function of rotation angle, for parallel and antiparallel magnetic alignment of the Ni contacts.

varies with θ for both parallel alignment and antiparallel alignment. It is clearly evident that the variation of the conductance with rotation angle is opposite for the two alignments: for parallel alignment the conductance decreases with angle, while for antiparallel alignment the conductance increases with angle. A crossover in the conductance occurs between 20° and 25° .

IV. CONCLUSIONS

We have investigated theoretically the spin-polarized transport properties of the 1,12-tri-benzene-dithiolate molecule coupled to two magnetic nickel contacts, focusing on the consequences of low-energy structural deformations for transport. We find that the current-voltage characteristics and magnetotransport properties are very sensitive to low-energy deformations in which one of the three benzene rings is rotated away from its equilibrium configuration. Specifically, we find that the total current (at fixed voltage) can be changed by factors of two or more for deformations costing of order 100 meV. The junction magnetoresistance is even more sensitive to molecular conformation, with changes even in the sign of the magnetoresistance expected for modest structural deformations. Recent experiments revealing the important role for molecular conduction played by conformation²⁸ strongly suggest that our theoretical findings are not unique to the system studied here, but indeed can be anticipated to be common to a large class of molecular-scale conductors.

ACKNOWLEDGMENTS

This work was supported by ONR, the NRC-NRL Associateship program, and the National Computational Science Alliance under Grant Nos. DMR050057 and DMR040044. Some computations were performed at the DoD Major Shared Resource Center at ASC.

*Electronic address: erwin@dave.nrl.navy.mil

- ¹A. Aviram and M. A. Ratner, *Chem. Phys. Lett.* **29**, 277 (1974).
- ²A. S. Martin, J. R. Sambles, and G. J. Ashwell, *Phys. Rev. Lett.* **70**, 218 (1993).
- ³M. A. Reed, C. Zhou, C. J. Muller, T. P. Burgin, and J. M. Tour, *Science* **278**, 252 (1997).
- ⁴J. Park, A. C. Pasupathy, J. I. Goldsmith, C. Chang, Y. L. Yaish, J. R. Petta, M. Rinkoski, J. P. Sethna, H. D. Abruna, P. L. McEuen, and D. C. Ralph, *Nature (London)* **417**, 722 (2002).
- ⁵W. Liang, M. P. Shores, M. Bockrath, J. R. Long, and H. Park, *Nature (London)* **417**, 725 (2002).
- ⁶J. R. Heath and M. A. Ratner, *Phys. Today* **56**, 43 (2003).
- ⁷A. Nitzan and M. A. Ratner, *Science* **300**, 1384 (2003).
- ⁸M. Schulz, *Nature (London)* **399**, 729 (1999).
- ⁹K. Tsukagoshi, B. W. Alphenaar, and H. Ago, *Nature (London)* **401**, 572 (1999).
- ¹⁰M. Ouyang and D. D. Awschalom, *Science* **301**, 1074 (2003).
- ¹¹Z. H. Xiong, D. Wu, Z. V. Vardeny, and J. Shi, *Nature (London)* **427**, 821 (2004).
- ¹²J. R. Petta, S. K. Slater, and D. C. Ralph, *Phys. Rev. Lett.* **93**, 136601 (2004).
- ¹³E. Emberly and G. Kirczenow, *Chem. Phys. Lett.* **281**, 311 (2002).
- ¹⁴M. Zwolak and M. DiVentra, *Appl. Phys. Lett.* **81**, 925 (2002).
- ¹⁵R. Pati, L. Senapati, P. M. Ajayan, and S. K. Nayak, *Phys. Rev. B* **68**, 100407(R) (2003).
- ¹⁶L. Senapati, J. Schrier, and K. B. Whaley, *Nano Lett.* **4**, 2073 (2004).
- ¹⁷L. Senapati, R. Pati, M. Mailman, and S. K. Nayak, *Phys. Rev. B* **72**, 064416 (2005).
- ¹⁸A. R. Rocha, V. M. García-Suárez, S. W. Bailey, C. J. Lambert, J. Ferrer, and S. Sanvito, *Nat. Mater.* **4**, 335 (2005).
- ¹⁹H. Dalglish and G. Kirczenow, *Phys. Rev. B* **72**, 184407 (2005).
- ²⁰M. Stamenova, S. Sanvito, and T. N. Todorov, *Phys. Rev. B* **72**, 134407 (2005).
- ²¹D. Waldron, P. Haney, B. Larade, A. MacDonald, and H. Guo, *Phys. Rev. Lett.* **96**, 166804 (2006).
- ²²R. G. Parr and W. Yang, *Density-Functional Theory of Atoms and Molecules* (Oxford Science, Oxford, 1994).
- ²³S. Datta, *Electron Transport in Mesoscopic Systems* (Cambridge University Press, Cambridge, 1997).
- ²⁴Gaussian 03, Gaussian Inc., Pittsburgh, PA, 2003.
- ²⁵D. A. Papaconstantopoulos, *Handbook of the Band Structure of Elemental Solids* (Plenum, New York, 1986).
- ²⁶W. Tian, S. Datta, S. Hong, R. Reifenberger, J. I. Henderson, and C. P. Kubiak, *J. Chem. Phys.* **109**, 2874 (1998).
- ²⁷R. Pati and S. P. Karna, *Phys. Rev. B* **69**, 155419 (2004).
- ²⁸F. Moresco, G. Meyer, K. H. Rieder, H. Tang, A. Gourdon, and C. Joachim, *Phys. Rev. Lett.* **86**, 672 (2001).
- ²⁹B. Y. Choi, S. J. Kahng, S. Kim, H. Kim, H. W. Kim, Y. J. Song, J. Ihm, and Y. Kuk, *Phys. Rev. Lett.* **96**, 156106 (2006).
- ³⁰M. Paulsson, T. Frederiksen, and M. Brandbyge, *Nano Lett.* **6**, 258 (2006).